Enz, J.; Riekehr, S.; Ventzke, V.; Kashaev, N.:

Influence of the Local Chemical Composition on the Mechanical Properties of Laser Beam Welded Al-Li Alloys

In: Physics Procedia (2012) Elsevier

DOI: 10.1016/j.phpro.2012.10.013

Influence of the Local Chemical Composition on the Mechanical Properties of Laser Beam Welded Al-Li Alloys

Josephin Enz*, Stefan Riekehr, Volker Ventzke, Nikolai Kashaev

Helmholtz-Zentrum Geesthacht, Institute of Materials Research, Materials Mechanics / ACE Centre, Max-Planck-Straße1, 21502 Geesthacht, Germany

Abstract

The increasing interest of the aircraft industry in reduction of structural weight of aircrafts has resulted in the development of lightweight and high-strength Al-Li alloys as well as in the introduction of laser beam welding to the manufacturing process. The objective of this study is the investigation of the influence of variations in the chemical composition on local mechanical properties, like micro-hardness and micro-tensile strength, of CO_2 laser beam welded skin-stringer joints made from AA2196 and AA2198. Additionally the influence of the welding process on weld chemistry is studied in view of the improvement of the weld quality.

Keywords: CO_2 laser beam welding; high strength aluminium alloys; Al-Li; decomposition behaviour; micro-tensile test

1. Motivation and State of the Art

The recently developed Al-Li alloys AA2196 and AA2198 are very promising lightweight and high-strength alloys for applications in the aircraft industry. For example, they can be used for skin-stringer joints of fuselage panels. Laser beam welding (LBW) of skin-stringer joints is already an established process for aircraft manufacturing which offers further weight savings by replacing the riveted differential structure by a welded integral structure [1]. However, Al-Li alloys typically show weldability problems mainly due to the hot cracking sensitivity and the formation of porosity which usually results in a degradation of the mechanical properties of the joints [2]. Besides this, the welding of lithium-bearing aluminium alloys results in the formation of two apparently differing phases [3] whose influence on the mechanical properties is until now not clarified. For this reason the influence of the local chemical composition on the mechanical properties will be investigated in this study. Additionally the influence of the alloy combination and the welding process on the formation of these phases will be studied in view of the improvement of the weld quality.

* Corresponding author. Tel.: +49-4152-87-2507; fax: +49-4152-87-42507.
E-mail address: josephin.enz@hzg.de.

2. Materials and Experimental Procedures

2.1. Aluminium-Lithium Alloys

Al-Li alloys, like the new alloys AA2196 and AA2198 of the third generation, feature a low density and a high strength at the same time which corresponds to the demands of the aircraft industry for materials of fuselage panels. In addition, a good weldability of these alloys is also essential for the manufacturer, because this allows the production of light integral structures. The properties of the Al-Li welds strongly depend on the welding preparation and also on the welding process.

Two different alloy combinations of skin and stringer, AA2198-AA2196 (A) and AA2198-AA2198 (B), were joined by laser beam welding in order to study the influence of the base materials on the weld formation. The combination A is the intended alloy combination of the material producers for the fuselage structure.

The skin used in this study, a 5.0 mm thick rolled plate, was made from the alloy AA2198 in the T3 heat treatment condition. The stringer for combination A, a 3.0 mm thick extruded profile, was made from the alloy AA2196 in the T8 condition. Whereas the stringer for combination B, a 1.9 mm thick rolled plate, was also made from the alloy AA2198 in the T3 condition. This stringer alloy possesses a higher strength than the skin alloy, which is needed for stiffening the fuselage structure. The chemical compositions of the Al-Li alloys used for this study are given in Table 1.

Since age hardenable aluminium alloys tend to develop metallurgical induced hot cracks in the weld seam, the skin-stringer joint has to be welded with additional filler wire, which possesses a high Si-content to compensate the crack formation [1]. In this study a filler wire made of AA4047 (see Table 1) with a diameter of 0.8 mm was used.

Table 1. Chemical composition (wt %) of the used aluminium alloys

Alloy	Si	Fe	Cu	Mn	Mg	Cr	Zn	Ti	Ag	Li	Zr	Al
AA2196 (stringer)	0.03	0.06	2.88	0.32	0.34	0.01	0.02	0.02	-	1.7	0.11	bal.
AA2198 (skin)	0.03	0.05	3.33	0.03	0.32	0.05	0.02	0.02	0.27	0.98	0.14	bal.
AA4047 (filler wire)	12.0	0.8	0.3	0.15	0.1	-	0.2	-	-	-	-	bal.

Like all aluminium alloys, the Al-Li alloys develop an oxide film on the surface whose growth rate is even increased by the existence of lithium as alloying element. This oxide film is mainly responsible for the formation of porosity in the weld seams. Hence, a surface preparation in the joining zone was accomplished by mechanically milling followed by cleaning with ethanol. For this purpose a surface layer of at least 150 µm was removed directly before welding.

2.2. Laser Beam Welding

The welding was performed using a large scale laser welding facility equipped with a movable processing head (see Figures 1a and 1b) and two 3.5 kW CO_2-lasers (with beam quality $K \approx 0.76$, beam parameter product BPP = 4.4 mm mrad and beam focus diameter $d \approx 130$ µm). The facility has been installed in cooperation with AIRBUS Germany. It facilitates an up-scaling of the welding process from coupon specimens up to complete fuselage panels with dimensions of 8500 mm x 3000 mm. In addition, this facility allows an easy implementation of the developed welding process to industrial manufacturing of aircraft components.

The T-joints of skin and stringer were welded simultaneously from both sides of the stringer as well as successively from each side of the stringer. The incident beam angle of both lasers was constantly at 22°. The filler wire AA4047 and the shielding gas helium were supplied from each side of the stringer in front feeding mode. The welding equipment and joint configuration used in this study are shown in Figure 1c. To retain the position of skin and stringer during welding a vacuum unit for the skin and a mechanical clamping device for the stringer were used.

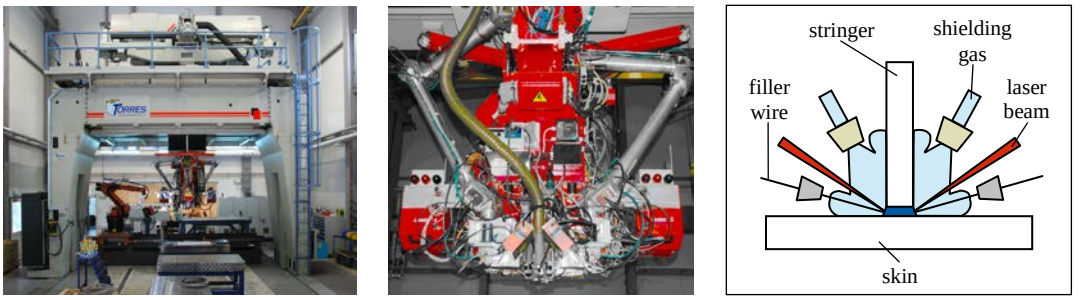

Fig. 1. Laser welding facility (a) with laser processing head (b) and schematic diagram of the joint configuration (c)

The welding sequence (simultaneous or successive welding) and parameter sets (laser power, welding speed, filler wire feed rate) used for welding were varied for both alloy combinations A and B (see Table 2). The welding parameter sets were analyzed with regard to porosity and good weld seam formation by the use of design of experiments.

Table 2. Welding parameter ranges for both alloy combinations

Alloy combination (skin-stringer)	Laser power P_W	Welding speed v_w	Filler wire feed rate v_{fw}	Welding sequence
AA2198-AA2196 (A)	1.80-2.00 kW	5.0-6.0 m/min	6.0-8.0 m/min	simultaneous/successive
AA2198-AA2198 (B)	1.48-1.72 kW	3.8-6.2 m/min	7.0-9.0 m/min	simultaneous/successive

2.3. Determination of the Microstructural, Chemical and Mechanical Properties

The microstructures and the phase formation of the welds of both alloy combinations were analyzed by optical microscopy. Therefore the microsections of the welds were grinded, polished and then etched with Keller's reagent.

Selected welds were investigated by the use of the scanning electron microscope (SEM) on unetched microsections and the local chemical composition (except Li) was analyzed by the energy dispersive X-ray (EDX) analysis (see Figure 2a). The local Li-content was measured in 0.3 mm thick layers of the weld by inductively coupled plasma atomic emission spectroscopy (ICP-AES) with previous acid hydrolysis (see Figure 2b). Therefore 10 layers were successively removed by mechanical milling and the chips of each layer collected and analyzed. The measured Si- and Li-contents were compared to calculated theoretical values. For the calculation of the theoretical content C_{th} of Si and Li in the weld equation (1) was used, with the cross-sectional area A and the content C of the base materials of skin, stringer and filler wire, assuming a homogeneous dilution of base materials (see Figure 2c). Because of differences between welding speed and filler wire feed rate, the diameter of the filler wire was adjusted with the help of equation (2).

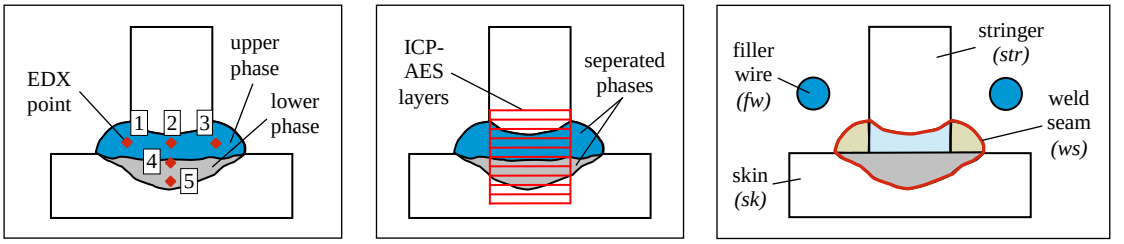

Fig. 2. Schematic diagram of the position of measuring points for the EDX analysis in the separated phases (a), of the position of measuring layers for the ICP-AES analysis (b) and of cross-sectional area for the calculation principles (c)

$$C_{th,Si/Li} = \frac{A_{sk} \cdot C_{Si/Li,sk} + A_{str} \cdot C_{Si/Li,str} + 2 \cdot \overline{A_{fw}} \cdot C_{Si/Li,fw}}{A_{ws}} \tag{1}$$

$$\overline{A_{fw}} = \frac{A_{fw} \cdot v_{fw}}{v_w} \tag{2}$$

The local mechanical properties of the welds were determined in two different ways. In the first, Vickers micro-hardness measurements (HV 0.2) were performed on etched microsections to identify the different phases. Therefore a grid pattern with 0.3 mm grid spacing was chosen. And in the second, micro-tensile tests were performed, which has been introduced by [4]. The 0.5 mm thick flat micro-tensile specimens (see Figure 3a) were extracted from the welds via electro discharge machining longitudinal to the welding direction. Since the width of the specimens is slightly greater than the width of the stringer after the mechanically milling, it was not possible to extract specimens from the stringer (see Figure 3b). They were tested on a Zwick 2.5 kN testing machine. Both test procedures allow distinguishing between the mechanical properties of different phases.

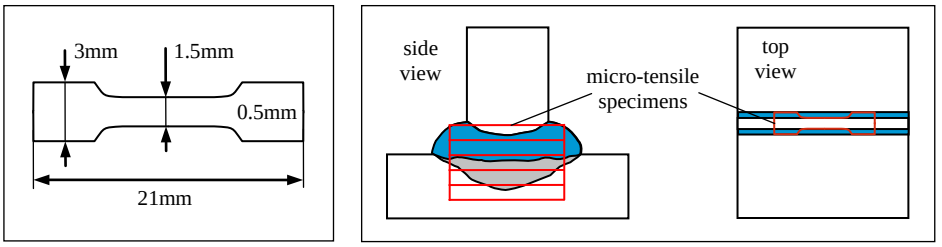

Fig. 3. Schematic diagram of the dimensions (a) and the extraction (b) of the flat micro-tensile specimens

3. Results and Discussion

3.1. Microstructure of the Welds

A phase separation was observed in all examined microsections for both alloy combinations A and B. The phase separation appears as a different etching behaviour which indicates a differing chemical composition. The upper phase showed in comparison to the lower phase a more light-coloured appearance with considerable flow marks which indicate an inhomogeneous solidification in this area (see Figures 4a and 4b). The different chemical composition is attended by an atypical grain growth. The atypical grain

growth is in turn characterized by less dendritic grains which are locally agglomerated (see Figure 4c). By variation of the welding sequence and the welding parameter sets by the use of design of experiments no definite dependence of the welding parameters on the phase separation behaviour was observed. It was always impossible to achieve a perfect dilution of the base materials of skin, stringer and filler wire. For this reason the dilution seems to be affected by other parameters which are hard to control or cause process instabilities, respectively.

In addition, all examined microsections showed porosity, which can not be removed completely, but reduced significantly by a proper surface preparation of the weld zone and the variation of the weld parameter sets. Some of the microsections also show cracks which lie along the solidification front of the atypical grains. This type of cracks can also indicate a loss of Si in this area.

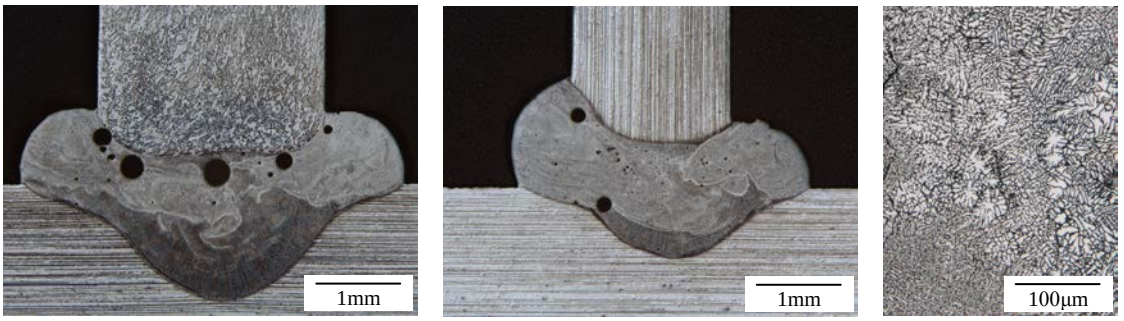

Fig. 4. Observed phase separation in alloy combination AA2198-AA2196 (A) (a) and AA2198-AA2198 (B) (b) and exemplary atypical grain growth in the upper phase observed in both alloy combinations (c)

3.2. Local Chemical Composition of the Welds

The EDX-analysis of the welds shows that there is an inhomogeneous distribution of alloying elements in the weld. In lower phase heavy elements like Cu and Ag are accumulated whereas in the upper phase light elements like Si were found. The measured values for an exemplary weld of alloy combination A are shown in Table 3. Within the upper phase the content of Si, which was mainly brought into the weld by the filler wire, also varies a lot. The outer areas of the upper phase (positions 1 and 3 in Figure 2a) show a higher Si-content in comparison to the centre of this phase (position 2 in Figure 2a). However, the Si-content measured in the welds is always lower than the theoretical calculated value according to equation (1). For example, for a calculated Si-content of 2.5 wt % in a weld of alloy combination A only a maximum value of approx. 1.6 wt % was measured (see Table 3). This indicates an insufficient dilution and a considerable loss of Si during welding. A value of around 0.8 wt % Si leads to a high hot cracking sensitivity. To avoid hot cracking of the weld, a Si-content of at least 2 wt % is needed [5].

Table 3. Content of the alloying elements (wt %) at 5 positions within a weld seam (according to Figure 2a) of alloy combination AA2198-AA2196 (A) measured by EDX (not determinable *)

Position in the weld seam	Phase	Measured value for alloying element content						
		Al	Cu	Si	Ag	Fe	Mg	Zr
1	upper	92.31	5.20	1.62	0.49	0.37	*	*
2	upper	93.53	5.13	0.55	0.49	*	*	0.29
3	upper	93.03	5.08	1.47	0.32	*	0.11	*
4	lower	92.78	6.40	*	0.47	0.35	*	*
5	lower	90.56	8.62	*	0.66	*	0.16	*

Since it is impossible to measure the Li-content in the weld via EDX-analysis the ICP-AES was used which has a lower resolution. By the use of this method, it is shown that there is also an inhomogeneous distribution of Li in the weld. The measured values are shown in Table 4. The lowest Li-contents were measured in layer below the stringer (marked light grey in Table 4). These values are slightly below the theoretical calculated values according to equation (1). This indicates a small loss of Li during welding. The Li-content of the lower phase is close to the Li-content of base material of the skin. This in turn indicates an insufficient dilution of the base materials. It should be mentioned that a marginal falsification of the results exists, because not only the weld but also a small volume of base material was measured (see Figure 2).

Table 4. Li-content (wt %) in 10 layers of the weld of both alloy combinations measured by ICP-AES in comparison to the theoretical calculated values (base material of stringer * and skin **)

Alloy combination (skin-stringer)	Theoretical calculated value	Measured value in position relative to skin surface (mm)									
		+1.2 *	+0.9	+0.6	+0.3	-0.3	-0.6	-0.9	-1.2 **	-1.5 **	-1.8 **
AA2198-AA2196 (A)	1.0	1.70	1.66	1.53	1.02	0.94	1.04	1.06	1.04	1.02	0.98
AA2198-AA2198 (B)	0.7	0.95	0.83	0.77	0.64	0.70	0.89	0.98	1.00	1.00	1.00

One possible reason for the insufficient dilution of the molten material and the formation of phases could be an unfavorable melt pool dynamic caused by the highly volatile alloying elements Mg and Li which have a vapor temperature close to the melting temperature of the alloy [6].

3.3. Local Mechanical Properties of the Welds

For both alloy combinations the lowest micro-hardness of 50-80 HV 0.2 was mainly measured in the upper phase of the weld. In contrast, the highest micro-hardness of 160 HV 0.2 was measured in the AA2196 stringer of alloy combination A. However, the average micro-hardness in the weld seam of this alloy combination is approx. -30 HV 0.2 lower as compared to alloy combination B distribution (see Figures 5a and 5b). And the latter has compared to alloy combination A as well a more homogeneous micro-hardness.

The micro-tensile tests with 0.5 mm, 1-dimensional increments have a lower resolution compared to the micro-hardness test with 0.3 mm, 2-dimensional increments. But the lowest tensile strength with 70-260 MPa for both alloy combinations was as well measured in the upper phase of the weld. The alloy combination A possesses again a considerably lower tensile strength in the weld compared to alloy combination B, although the AA2196 stringer has a higher tensile strength compared to the AA2198 stringer. The alloy combination B has also a quite homogenous distribution of the local tensile strength (see Figures 5a and 5b).

From the described results it can be assumed that the micro-hardness and the micro-tensile strength are affected by the chemical composition of the weld, of course, besides the changed temper condition due to the welding process. In the upper phase of the weld, where inferior mechanical properties occur, the Si-content is supposed to be close to the critical value for hot cracking and as well the Li-content is lower compared to the base material. Both (but especially the low Si-content) can lead to a degradation of the local mechanical properties of the weld. And the same applies for the presence of porosity in the weld. In [7] it has been already shown that also the macroscopic mechanical properties of the more homogeneous welds of alloy combination B are superior compared to alloy combination A with an AA2196 stringer.

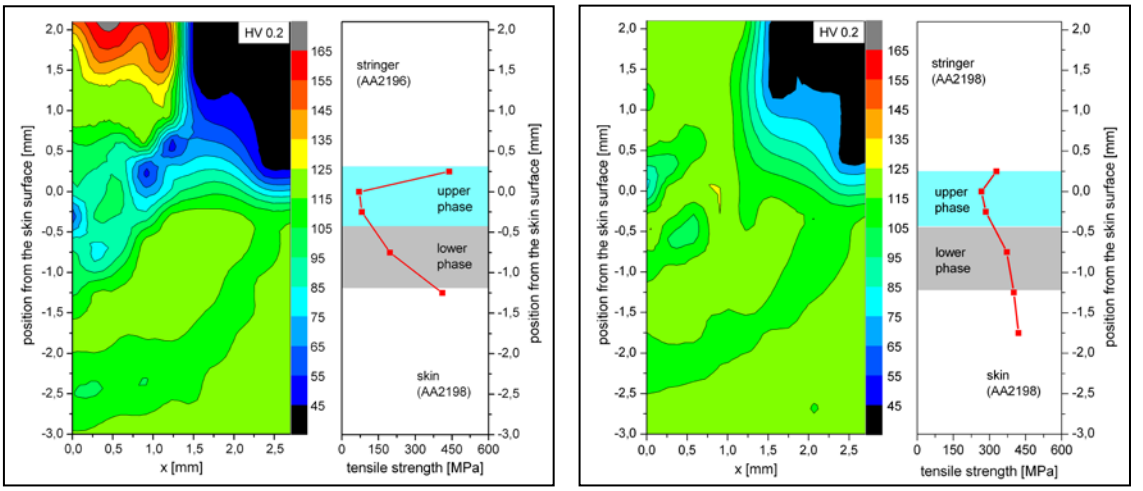

Fig.5. Distribution of the micro-hardness in the weld seam and micro-tensile strength of different layers of the weld for alloy combination AA2198-AA2196 (A) (a) and AA2198-AA2198 (B) (b)

4. Conclusion

The attained results of this study show a measurable influence of the local chemical composition on the mechanical properties of an Al-Li weld. The chemical composition of a weld is defined by the alloy combination but it is also changing within the weld seam due to the phase separation and the insufficient dilution of the molten base materials, respectively. To avoid a mechanical degradation of the welds a good dilution has to be considered during the LBW process of Al-Li alloys. The inhomogeneous distribution of Li in the weld yields in local hardness and strength differences. Whereas the local loss of Si during welding causes hot cracking whose influence on the mechanical properties of the welds is supposed to be greater. The influence of the distribution of the alloying elements by the welding process (e.g. welding sequence and parameter changes) is not obvious and it is additionally limited due to the formation of defects like pores and cracks for particular parameter sets.

References

[1] Dittrich, D.; Standfuss, J.; Liebscher, J.; Brenner, B.; Beyer, E.: Laser Beam Welding of Hard to Weld Al Alloys for a Regional Aircraft Fuselage Design – First Results. *Physics Procedia.* 2011; **12**: pp. 113–122.

[2] Kostrivas, A.; Lippold, J.C.: Weldability of Li-bearing Aluminium Alloys. *Internations Materials Reviews*. 1999; **44** [6], pp. 217-237

[3] Soni, K.K.; Shah, S.; Gentz, S.: SIMS imagin of Al-Li alloy welds. *Advanced Materials & Processes.* 1996; **149** [4]: pp. 35-36

[4] Çam, G.; Yeni, Ç.; Erim, S., Ventzke, V.; Koçak, M.: Investigation into Properties of Laser Welded Similar and Dissimilar Steel Joints. *Science and Technology of Welding and Joining*. 1998; **3** [4]: pp. 177-189

[5] Lippold, J.; Böllinghaus, T.; Cross, C.E.: *Hot Cracking Phenomena in Welds*. Vol.3. Springer Verlag. 2011

[6] Schinzel, C.M.: *Nd:YAG-Laserstrahlschweißen von Aluminiumwerkstoffen für Anwendungen im Automobilbau*. Utz Verlag. 2002

[7] Enz, J., Riekehr, S.; Ventzke, V.; Kashaev, N.; Huber, N.: *Prozessoptimierung für das Laserstrahlschweißen von hochfesten Aluminium-Lithium-Leigerungen*. Accepted for publication in Welding and Cutting, DVS Verlag. 2012